EARTHQUAKE SPECTRA

The Professional Journal of the Earthquake Engineering Research Institute

PREPRINT

This preprint is a PDF of a manuscript that has been accepted for publication in *Earthquake Spectra*. It is the final version that was uploaded and approved by the author(s). While the paper has been through the usual rigorous peer review process for the Journal, it has not been copyedited, nor have the figures and tables been modified for final publication. Please also note that the paper may refer to online Appendices that are not yet available.

We have posted this preliminary version of the manuscript online in the interest of making the scientific findings available for distribution and citation as quickly as possible following acceptance. However, readers should be aware that the final, published version will look different from this version and may also have some differences in content.

The DOI for this manuscript and the correct format for citing the paper are given at the top of the online (html) abstract.

Once the final, published version of this paper is posted online, it will replace the preliminary version at the specified DOI.

Seismic Reliability Assessment of Aging Highway Bridge Networks with Field Instrumentation Data and Correlated Failures. II: *Application*

Keivan Rokneddin,[a] **Jayadipta Ghosh,**[a] **Leonardo Dueñas–Osorio,**[a] **and Jamie E. Padgett**[a]

The Bridge Reliability in Networks (BRAN) methodology introduced in the companion paper is applied to evaluate the reliability of part of the highway bridge network in South Carolina, USA, under a selected seismic scenario. The case study demonstrates Bayesian updating of deterioration parameters across bridges after spatial interpolation of data acquired from limited instrumented bridges. The updated deterioration parameters inform aging bridge seismic fragility curves through multi-dimensional integration of parameterized fragility models, which are utilized to derive bridge failure probabilities. The paper establishes the correlation structure among bridge failures from three information sources to generate realizations of bridge failures for network level reliability assessment by Monte Carlo analysis. Positive correlations improve the reliability of the case study network, also predicted from the network topology. The benefits of the BRAN methodology are highlighted in its applicability to large networks while addressing some of the existing gaps in bridge network reliability studies.

INTRODUCTION

Network level bridge reliability studies provide critical information for risk assessment and life-cycle cost analysis of bridges in transportation systems. Specifically, seismic reliability assessment of bridge networks helps the owners of transportation systems make informed decisions on post-event accessibility of critical points in the network, estimate losses from seismic scenarios, or evaluate the criticality of bridges for maintenance and retrofit prioritization.

Earthquakes have historically caused considerable damage to highway bridge systems. For example, events such as the 1989 Loma Prieta (Board et al. 1994), 1994 Northridge (Schiff

---

[a] Department of Civil and Environmental Engineering, Rice University, Houston TX 77005

1995), 1995 Kobe (Chang 2000), and more recently the 2008 Sichuan (Han et al. 2009) earthquakes provided widespread evidence of the vulnerability of highway bridges to seismic events and the socio-economic impacts associated with their collapse. The potential vulnerability of highway bridges to seismic events is further exacerbated because the majority of the bridges are nearing the end of their service life and affected by the effects of aging and deterioration, as reported for the United States (ASCE 2009).

The Bridge Reliability Assessment in Networks (BRAN) methodology, presented in the companion *Methodology* paper, improves upon the existing literature in highway bridge system reliability research by: a) incorporating data from field monitoring of deteriorating highway bridges in networks to estimate aging bridge reliabilities using parameterized fragility models, and b) assessing the network-level reliability while explicitly considering correlations among bridge failures. The current *Application* paper implements this methodology to part of the bridge network in the state of South Carolina, USA, to evaluate its connectivity reliability for a defined seismic scenario. The bridge failure probabilities are computed for the extensive damage state for which long term bridge functionality is impaired. The case study transportation system surrounds the state capital in Charleston with important facilities and urban infrastructure, and expands over an active seismic zone where a significant historic seismic event occurred in 1886. Over 83% of the bridges in the network belong to the category of non-seismically designed bridges (pre-1990 construction), and have been characterized by previous researchers as seismically vulnerable (Nielson and DesRoches 2007). Additionally, highway bridges in this network are over 40 years old on average and hence, susceptible to aging and deterioration mechanisms which affect seismic vulnerability, as confirmed in a recent study by Rokneddin et al. (2011). Previous studies on the seismic vulnerability of highway bridges in the region highlight potential bridge susceptibility (e.g. Wong et al. 2005; Padgett et al. 2010); however, they do not consider the effects of aging and network-level performance.

The paper is organized as follows: the next section introduces the test bed transportation system by elaborating on the existing bridge classes and topological characteristics of the network. The following two sections (Stage A of BRAN methodology) discuss the modeling of aging highway bridge fragilities in the network. Deterioration parameters across all bridges are updated after conducting spatial interpolation of available field-acquired data for only a limited number of bridges. Then, parameterized fragility models are developed to compute aging bridge

failure probabilities for the selected seismic scenario. To evaluate the network reliability (Stage B), a correlation structure is formed to represent dependencies among bridge failure probabilities and is used along with the computed bridge failure probabilities to generate samples for an efficient Markov Chain Monte Carlo network reliability algorithm. The final section presents results and discussions that reveal the impacts of deterioration parameter updating and different levels of correlations on network reliability. The paper ends with conclusions and future research opportunities.

DESCRIPTION OF THE CASE STUDY BRIDGE NETWORK

Figure 1 shows the case study highway bridge network in South Carolina, USA, along with the peak ground acceleration (PGA) contours resulting from a strong ground motion scenario of $M_w = 7.3$, based on the largest contributing event to the 10% exceedance probability in 50 years seismic de-aggregation map of the region (USGS 2010). The event's epicenter coincides with the epicenter of the historic 1886 Charleston earthquake, which is 20 km away from the center of Charleston. The PGA contours are computed using HAZUS-MH MR4 (FEMA 2009) with the weighted average of four attenuation relationships for central and eastern US, namely Atkinson and Boore (1995), Toro et al. (1997), Frankel et al. (2002), and Campbell (2003). The case study network lies in the greater Charleston area and includes bridges and roads along freeways, highways, and main roads encompassing the counties of Charleston, Berkeley, Orangeburg, Dorchester, and Colleton between Interstate-95 and the Atlantic Ocean.

The bridge inventory is obtained from the National Bridge Inventory (FHWA 2010) and integrated with the GIS map of the region's roadways from TELEATLAS (2010). The bridge network consists of a total of 509 highway bridges of nine different bridge classes categorized according to structure, material properties, and construction type (Table 1). The majority of these bridges do not include seismic detailing, and are also prone to the adverse effects of aging and deterioration given their age and proximity to the sea. A primary degrading agent, as elaborated in the companion *Methodology* paper, is airborne marine chlorides from the adjoining sea coast leading to corrosion deterioration of both exposed and embedded steel members. Two different marine exposure conditions are considered based on proximity to sea coast: a) marine splash zone for bridges located within 30ft (10m) from the sea coast, and b) marine atmospheric

exposure for other bridges. The case study network shows 30 out of the 509 bridges to be in the marine splash zone exposure.
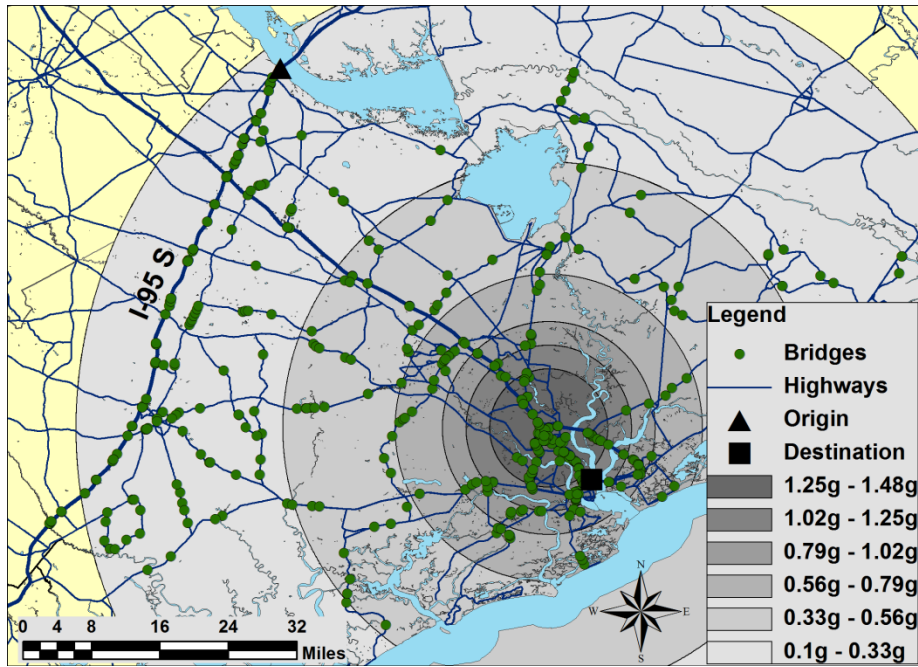

Figure 1. The case study area in the South Carolina transportation network. Origin and destination nodes for network reliability are shown, and PGA contours resulting from the selected seismic scenario are also depicted.

Table 1. Inventory of bridges in the case study transportation network showing the different classes

Bridge Classes	Number
MSSS Slab	159
MSSS Steel Girder	123
MSSS Concrete Girder	117
MSC Steel Girder	38
MSC Slab	17
SS Concrete	19
SS Steel	19
MSC Concrete Box Girder	15

MSC = Multi-span continuous, MSSS = Multi-span simply supported, SS = Simply supported

This study models bridges as nodes and roads as connecting links for network representation of the highway bridge system. The network topology is identified by an adjacency matrix (**A**), which is a square matrix of size equal to the number of nodes in the network. Each entry A_{ij} is equal to 1 if there is a direct link connecting node j to node i, and 0 otherwise. The authors

previously studied the same region for seismic network reliability and ranking of priority bridges (Rokneddin et al. 2011). However, the topological layout and associated matrix A of the current network differs from the previous study to avoid the formation of high degree nodes (nodes with many links attached). The existence of certain local roads without bridges in the former adjacency matrix provided alternative direct routes between pairs of bridges in the network, and hence, increased network accessibility. Although the layout with high-degree nodes is valid, the existence of such nodes challenges the conception that road networks are roughly mesh-like topological structures (i.e. grids). Furthermore, node degrees influence the criticality of nodes in importance measures that consider network topology. To address these concerns, all road intersections without a bridge that provide alternative routes in the current layout are equipped with virtual nodes in the current network layout to partition them and eliminate direct links. These virtual nodes do not represent bridges, and only affect the formation and size of the new adjacency matrix to conform to mesh topologies seen in practice. Consequently, the average node degree in the current network layout is equal to 2.65. Moreover, nodes have a maximum degree of 6, comparable to values from mesh-like road network topologies.

SPATIAL INTERPOLATION AND BAYESIAN UPDATING OF DETERIORATION PARAMETERS

SPATIAL INTERPOLATION OF DETERIORATION PARAMETERS

Accurate estimates of aging highway bridge fragilities for all bridges in the network require up to date information on deterioration parameters at all bridge locations. Since it is impractical to field-monitor every bridge in the transportation network, spatial interpolation techniques are employed to estimate the values of deterioration parameters for non-instrumented bridges from data made available by a limited number of instrumented bridges. This research applies the Kriging methodology for spatial interpolation, providing a simple yet efficient method to incorporate the correlation structure among observations while making predictions at unobserved locations. Since field instrumentation of bridges is considered to be an expensive and labor intensive procedure in practice, the number of bridges chosen for demonstration as 'field instrumented' is restricted to 100 out of the total 509 bridges in the network. The number of the sample points is consistent with the findings of Webster and Oliver (2008) and

Trauth et al. (2010), who recommend a minimum of 100 sample points for the construction of an appropriate variogram. Field instrumentations at each of the 100 bridge locations are assumed to gather data for the following deterioration parameters: 1) Surface chloride concentration (C_s), 2) Chloride diffusion coefficient (D_c), and 3) Corrosion rate (r_{corr}). Along with the concrete cover depth, these parameters are the key elements used to predict the corrosion initiation time and rate of area loss of steel. Following other corrosion deterioration studies (Enright and Frangopol 1998, 1999), the deterioration parameters at monitored bridge locations are assumed to follow lognormal distributions with hypothetical mean values assigned from the range of estimates reported in Table 2 (based on actual field measurements reported in literature) for the two deterioration zone exposure conditions. Additionally, based on available studies, the coefficient of variation (δ) of the distribution for both C_s and D_c is assumed to be 0.5 (Suzuki et al. 1990; Vu and Stewart 2000), while δ corresponding to r_{corr} lies between 0.14-0.33 (Thoft-Christensen 1995; Frangopol et al. 1997; Val et al. 1998; Vu and Stewart 2000).

Table 2. Range of mean values of deterioration parameters assigned to instrumented bridges and used for Kriging

Deterioration Parameter	Exposure Condition	Range of Parameter Estimate	Unit
C_s	Marine Splash	3.74 – 5.54[a]	% weight of cement
	Marine Atmospheric	0.43 – 2.22[b]	% weight of cement
D_c	Marine Splash	2.13 – 4.66[c]	10^{-12} m²/sec
	Marine Atmospheric	4.41 – 4.91[d]	10^{-12} m²/sec
r_{corr}	Marine Splash	0.22– 0.38[e]	mm/year
	Marine Atmospheric	0.05 – 0.10[e]	mm/year

[a]Funahashi (1990)   [b]Uji et al. (1990)   [c]Funahashi (1990) and Liam et al. (1992)   [d]Mustafa and Yusof (1994)
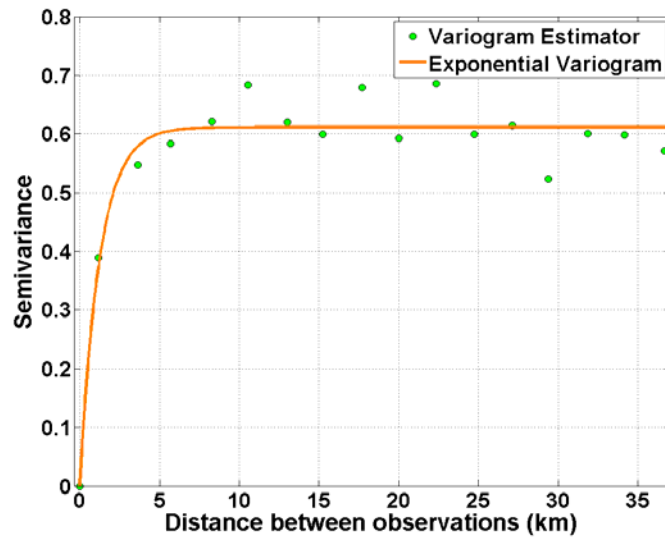[e]Zen (2005)

Figure 2. Exponential variogram for Kriging of surface chloride concentration across the network

The Kriging procedure involves constructing a variogram estimator from acquired data at instrumented bridge locations and subsequent variogram model fitting. Among several variogram models tested, the exponential model results in best goodness of fit estimates while fitting the variogram estimator and is thereby adopted in this study. Figure 2 exemplifies this model to predict the semivariance for surface chloride concentration C_s, which is used to calculate the Kriging weights and predict the mean surface chloride concentration at the remaining bridge locations. Figure 2 reveals that the spatial process is correlated over short distances while there is little spatial dependency for separation distances beyond 8 km (the "range" of the variogram). While the present case study uses only 100 out of 509 bridges for field instrumentation, the level of spatial dependency and the range of the variogram can be improved by increasing the number of instrumented bridges within the network. This further highlights the importance of instrumenting sufficient number of bridges within the network to obtain confident predictions. It is noted that the fitted variogram in Figure 2 results from one realization of the lognormal distribution for C_s at instrumented bridge locations, and therefore, the predicted estimates at the unobserved locations are only point estimates of C_s. The probability distribution of C_s at each bridge location is consequently formed by repeating this procedure N_{krig} times in a Monte Carlo scheme.
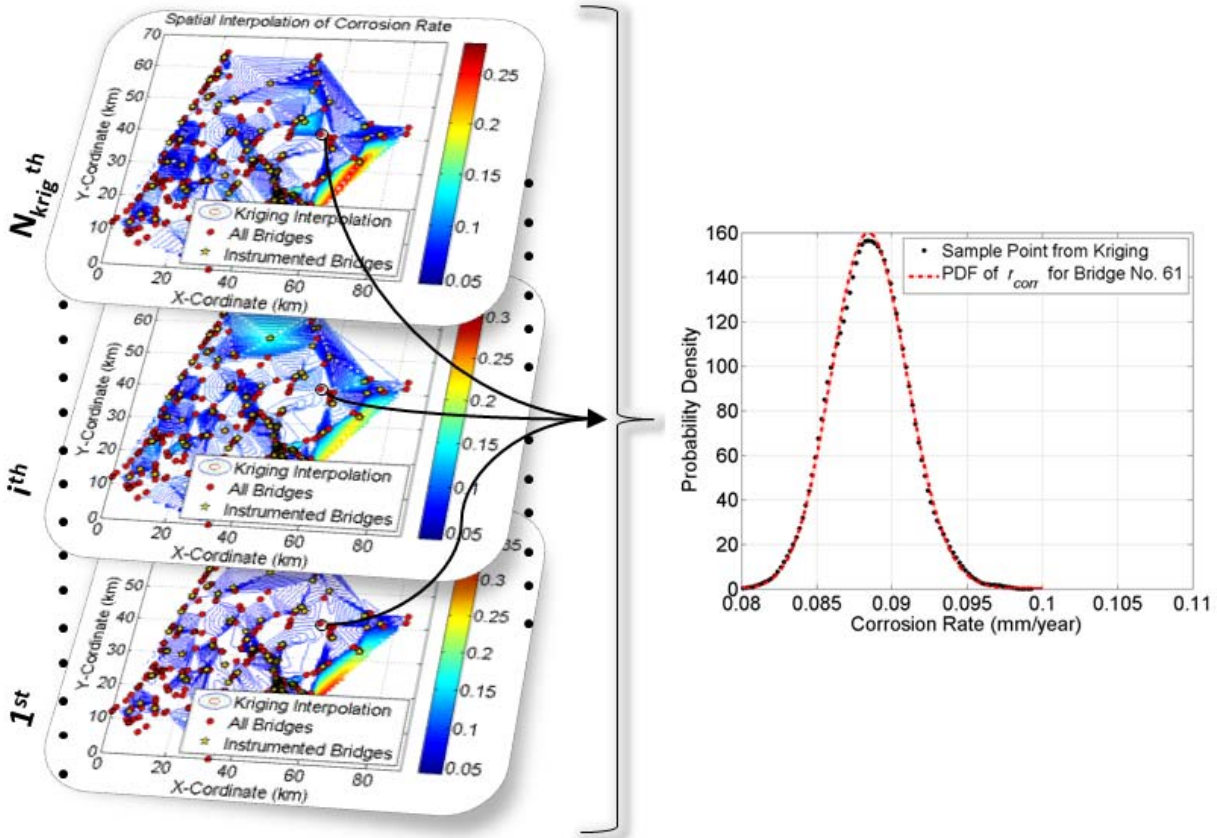
Figure 3. Repeated spatial interpolation of corrosion rate across the 509 bridge network using a Monte Carlo approach after drawing samples from the distribution of corrosion rate at instrumented bridge locations.

The same procedure applies to form the probability distributions of other deterioration parameters (D_c and r_{corr}). Figure 3 demonstrates the approach of repeated sampling and Kriging interpolation across the region to determine the distribution of r_{corr} at the specified unobserved bridge location. Both field acquired and estimated probability distributions of the deterioration parameters for all network bridges are regarded as new measurements, and are combined with historical estimates of deterioration parameters through Bayesian updating as discussed in the next section.
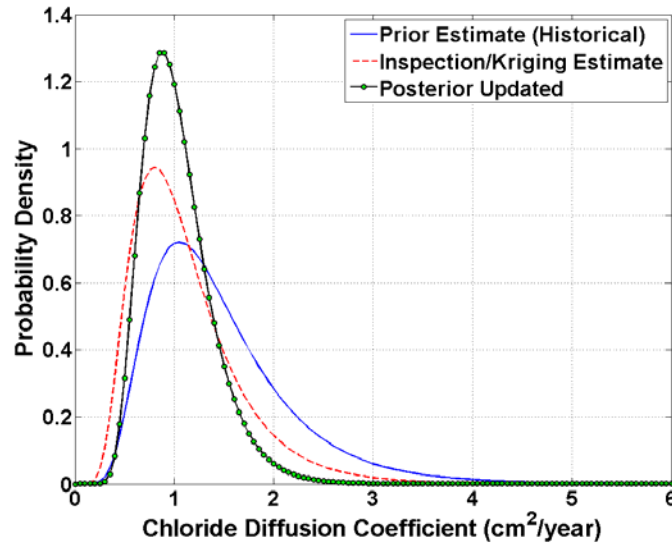
Figure 4. Bayesian updating example of chloride diffusion coefficient (D_c)

BAYESIAN UPDATING OF DETERIORATION PARAMETERS

The Bayesian updating technique provide a rational statistical approach to integrate the new information available from field instrumentation and historically available data from previous knowledge or experience to obtain more accurate probabilistic models of bridge conditions. The distribution of deterioration parameters representing "new information" constitute the likelihood function distribution at all bridge locations and are obtained after field instrumentation or spatial instrumentation of instrumented data, as elaborated in the preceding section. In this study, historical estimates of lognormal distributions of C_s and D_c, representing the prior distribution, are assumed to have mean values equal to the central values of the ranges outlined in Table 2 and the same coefficient of variation (δ) of 0.5. Additionally, the prior historic distributions of r_{corr} are obtained as a function of cover depth and water-cement ratio based on the equation proposed by Vu and Stewart (2000). Table 3 reports the mean values of prior distributions of the corrosion deterioration parameters considered in this study.

Table 3: Mean values of prior distributions of deterioration parameters representing historically available information

Deterioration Parameter	Exposure Condition	Prior Mean	Unit
C_s	Marine Splash	4.64[f]	% weight of cement
	Marine Atmospheric	1.33[f]	% weight of cement

D_c	Marine Splash	3.50^{f}	10^{-12} m²/sec
	Marine Atmospheric	4.66^{f}	10^{-12} m²/sec
r_{corr}	Marine Splash	Function of bridge age, cover depth and water-cement ratio (Vu and Stewart 2000)	mm/year
	Marine Atmospheric		mm/year

[f]Central value of ranges reported in Table 2

While the general formulation for Bayesian updating is presented in the companion *Methodology* paper, closed form solutions exist for typical distribution types (such as normal and lognormal distributions), which relaxes the computational complexity of the updating procedure (Ang and Tang 2007). Figure 4 shows an example of results of updating the lognormally distributed chloride diffusion coefficient, deriving a posterior estimate of D_c that incorporates both historic knowledge and field measurement data. Updated estimates of the deterioration parameters aid in determining the extent of deterioration of bridge structural members which eventually inform aging bridge fragility assessment. Similar Bayesian updating procedures are also performed for C_s and r_{corr}.

PARAMETERIZED BRIDGE FRAGILITY ASSESSMENTS

Present day seismic fragilities for all network bridges are estimated in this study by a parameterized fragility estimation approach. While the companion *Methodology* paper elaborates on general details of this approach for all bridge types, the fragility assessment of a specific bridge class in the network–MSSS concrete girder bridge–is presented to demonstrate its application. The parameterized fragility approach requires the development of surrogate demand models after identifying input vector x, which consists of: i) deterioration affected structural parameters as revealed from previous studies by Ghosh and Padgett (2010, 2012), and ii) critical bridge modeling parameters identified by Nielson (2005) following sensitivity studies on bridges located in Central and Southeastern US. These parameters are listed in Table 4 for the MSSS concrete girder bridge type.

DEVELOPMENT OF SURROGATE DEMAND MODELS

The response surface demand model provides a mathematical relationship between the dependent predicted values of a bridge component response and the independent predictor variables. The distinct advantage of such surrogate demand models lies in their flexibility to generate component specific demands given any combination of the input parameters without the need to conduct expansive computer simulations. The demand model fitting procedure begins with conducting nonlinear time-history analysis of finite element bridge models under earthquake loadings with bridge structural properties assigned from an experimental design matrix X obtained using the D-Optimal design strategy. For the experimental design procedure, the elements in input vector x are analyzed at five different levels with levels 1 and 5 (Table 4) corresponding to the minimum and maximum value of each design parameter. For the deterioration affected structural parameters (x_1 to x_4) levels 1 and 5 correspond to the pristine and severely deteriorated structural parameters, respectively, with the extent of deterioration computed using the aging models outlined in Ghosh and Padgett (2010, 2011). On the other hand, the upper and lower levels corresponding to the critical bridge modeling parameters (x_5 to x_7) are adopted from Nielson (2005). The three intermediate levels (levels 2, 3 and 4) are taken as the 25th, 50th, and 75th percentile of the uniformly distributed range of parameter space.

Table 4. Elements of input vector x consisting of deterioration affected structural parameters and critical bridge modeling parameters. Also presented in the table are the lower and upper levels of each parameter used to generate the experimental design matrix

Element in input vector x	Parameter Description	Unit	Lower Level (Level 1)	Upper Level (Level 5)
x_1	Column rebar area	cm^2	0.90	6.45
x_2	Elastomeric bearing dowel bar area	cm^2	0.55	5.09
x_3	Shear modulus of elastomeric bearing pads	MPa	0.10	6.0
x_4	Concrete cover depth	cm	0.00	10.16
x_5	Steel strength	MPa	275.79	517.11
x_6	Elastomeric bearing pad friction	%	10	150
x_7	Elastomeric bearing dowel gap	cm	0.00	5.08

Next, polynomial multilinear response surface metamodels are fitted to the component responses from nonlinear time-history analysis of bridge models, thereby providing a predictive relationship for the component responses based on the intensity of ground motion (*im*) and parameters x_1 to x_7. It is noted that the earthquake records used for the nonlinear time history analyses from the Wen and Wu (2001) and Rix and Fernandez (2004) ground motion suite has PGA intensities between 0.03 to 0.75g. While the adopted ground motions cover the lower range of intensity measure present in the network, it does not comply with the upper range. Consequently, component response estimations using the developed response surface models involve predictions for high PGA intensities beyond the original training set. A preliminary investigation conducted by the authors on the most popular bridge class (MSSS Slab) revealed that the extrapolated mean estimates using the developed metamodels are within satisfactory limits when compared to the predicted means from the metamodel fitted to the analysis data for original and scaled ground motions (to cover the wide PGA range in the network). While it is acknowledged that metamodels should be used with caution for extrapolations beyond the training set, the developed response surface metamodels for the unscaled original earthquake records are adopted with confidence based on the findings from the preliminary study.

Appropriate transformation of variables is often required in model fitting process to attain conforming multilinear response surface metamodels. While several forms of data transformations such as square-root transformation or inverse transformation exist, the logarithmic transformation (used in this study) is particularly helpful when the variable of interest ranges over several orders of magnitude (Shome and Cornell 1999; Cornell et al. 2002). The response surface metamodel adopted in this study is an extension of the seismic demand model proposed by Shome and Cornell (1999), including bridge parameters x_1 to x_7 in addition to *im* after pertinent variable transformation to the lognormal space. While the general form of the adopted metamodel is presented in the companion paper, the constant, linear and interaction coefficients pertaining to 8 different bridge component responses (Table 5) of the MSSS concrete bridge is available in the supplemental materials of this publication. The supplemental material also provides the response surface metamodel coefficients for other bridge classes analyzed in this study. The goodness of fit estimates - adjusted R^2 and mean squared error (*MSE*) - of the response surface model fitting for different bridge component responses of the MSSS concrete bridge are shown in Table 5. Although in general the response surface models provide a

good fit to the component response data, the adjusted R^2 values are relatively low for certain bridge components. Future studies will inspect other statistical learning techniques to improve the fit while capturing of the response of these bridge components. The generated response surface demand models will be used to generate bridge fragility curves as demonstrated in the subsequent section.

Table 5. Goodness of fit estimates for the multilinear response surface metamodels corresponding to different components of the MSSS Concrete girder bridge.

Component Number (k)	Component Response Description	Adjusted R^2	RMSE
1	Column curvature ductility	0.82	0.54
2	Fixed bearing deformation (Longitudinal)	0.76	0.69
3	Fixed bearing deformation (Transverse)	0.68	1.00
4	Expansion bearing deformation (Longitudinal)	0.77	0.59
5	Expansion bearing deformation (Transverse)	0.70	0.98
6	Abutment active deformation	0.65	0.50
7	Abutment passive deformation	0.66	0.83
8	Abutment transverse deformation	0.68	0.50

PARAMETERIZED FRAGILITY FORMULATION

Bridge component and system level fragility curves are derived in this study through logistic regression after constructing binary (survival/failure) vectors of Bernoulli trials for each of the critical bridge components listed in Table 5. The vectors of Bernoulli trials are formed by Monte Carlo simulations, comparing 50,000 point estimates of seismic demands (sampled from the component-specific metamodels) and capacities (sampled from the component-specific limit state distributions for the extensive damage state (Nielson and DesRoches (2007)) for random combinations of im and x_i's ($i = 1,...,7$). The system-level Bernoulli vector follows from the series system assumption, where the failure of any bridge component indicates system failure. Finally, logistic regression is conducted using the system-level Bernoulli vector to estimate bridge system failure conditioned on ground motion intensity and the bridge parameters x_1 to x_7,

as in Equation 1 for MSSS concrete bridges. The χ^2 goodness of fit test to assess the overall logistic regression model indicates excellent model fit with very low p-values (less than 10^{-4}).

$$p_{sys|im,x_1,x_2,...,x_7} = \frac{e^{6.15+4.00\log(im)-0.395x_1-0.116x_2+0.03\log(x_3)-0.148\log(x_4)-0.003x_5-0.251\log(x_6)-0.025\log(x_7)}}{1+e^{6.15+4.00\log(im)-0.395x_1-0.116x_2+0.03\log(x_3)-0.148\log(x_4)-0.003x_5-0.251\log(x_6)-0.025\log(x_7)}} \quad (1)$$

The parameterized fragility model presented in the form of Equation 1 has several advantages over 'classical' fragility curves conditioned only upon *im*. First, the probability of bridge failure for a given *im* can be found by simple substitution of parameters in Equation 1 if exact point estimates of the bridge parameters x_1 to x_7 are available. Second, the sensitivity of fragility estimates to any individual parameter or combination of different parameters can be studied by varying them while holding the remaining ones constant. Finally, if some, or all, of bridge parameters x_1 to x_7 are probabilistic in nature, one may estimate the fragility by integrating over the domain of the statistical distributions of the parameters. The next section exemplifies multi-dimensional integration for one particular MSSS concrete bridge in the network.

MULTI-DIMENSIONAL INTEGRATION OF PARAMETERIZED FRAGILITY MODELS

The multi-dimensional integration example presented here focuses on an MSSS concrete girder bridge built in 1922 and located in the marine atmospheric exposure zone. The field-instrumented/spatially interpolated and statistically updated deterioration parameters (C_s, D_c, and r_{corr}) derived from the techniques elaborated in the previous section are used to assess the extent of corrosion deterioration suffered by the column reinforcing bars and bearing dowel bars. Other forms of deterioration mechanisms encountered by this bridge include: increase in shear modulus of the elastomeric bearing pads due to thermal oxidation, and concrete cover spalling due to accumulation of rust products. Table 6 shows the statistical distributions of each of the deterioration affected structural parameters (x_1 to x_4) corresponding to the present day bridge conditions. Also shown in the table are the typical statistical distributions corresponding to critical bridge modeling parameters (x_5 to x_7) for MSSS concrete bridges located in the Central and Southeastern US as identified by Nielson (2005).

Table 6. Statistical distribution of the deterioration affected structural parameters (x_1 to x_4) and

critical bridge parameters (x_5 to x_7) corresponding to the case study MSSS Concrete Bridge

Parameter	Unit	Distribution Type	Distribution Parameters	
x_1	cm^2	Lognormal	$\lambda = 1.49$	$\zeta = 0.12$
x_2	cm^2	Lognormal	$\lambda = 1.36$	$\zeta = 0.11$
x_3	MPa	Uniform	$a = 1.37$	$b = 4.35$
x_4	cm	Lognormal	$\lambda = -4.65$	$\zeta = 0.29$
x_5	MPa	Lognormal	$\lambda = 6.13$	$\zeta = 0.08$
x_6	-	Lognormal	$\lambda = 0.00$	$\zeta = 0.10$
x_7	cm	Uniform	$a = 0.00$	$b = 5.08$

λ and ζ are parameters of the lognormal distribution. a and b are the support parameters of the uniform distribution.

Single-parameter fragility curves for the example bridge conditioned only on *im* are estimated by integrating the multi-dimensional fragility estimates over the domain of the uncertainties for the different parameters as shown in Equation 2. This fragility curve (Figure 5) thus obtained, is similar to a 'classical' fragility curve, although it incorporates all the effects of aging and deterioration and their associated uncertainties. It is noted that parameters x_1 to x_7 are assumed to be statistically independent which enables the multi-dimensional integration over each parameter specific distribution without constructing the joint probability density function.

$$p_{sys|im} = \int_{x_1} ... \int_{x_7} \frac{e^{6.15+4.00\log(im)-0.395x_1-0.116x_2+0.03\log(x_3)-0.148\log(x_4)-0.003x_5-0.251\log(x_6)-0.025\log(x_7)}}{1+e^{6.15+4.00\log(im)-0.395x_1-0.116x_2+0.03\log(x_3)-0.148\log(x_4)-0.003x_5-0.251\log(x_6)-0.025\log(x_7)}} f(x_1)...f(x_7)dx_1...dx_7 \quad (2)$$

The fragility curves derived using the proposed parameterized formulation and subsequent multi-dimensional integration are compared with the traditional state-of-the-practice method for fragility analysis. In the conventional method, surrogate demand models conditioned only on *im* are developed using component responses obtained from finite element analysis of bridge samples constructed through Latin Hypercube sampling of deterioration and modeling parameters. Finally, the derived fragility curve is characterized by a lognormal distribution with a median and dispersion value. This practical fragility development method has been widely adopted by researchers to determine analytical fragility curves for as-built pristine bridges (Choi et al. 2004; Nielson and DesRoches 2007; Kim and Shinozuka 2004; Mackie and Stojadinovic 2006), seismically retrofitted bridges (Padgett and DesRoches 2009), and recently for deteriorating highway bridges (Ghosh and Padgett 2010). As elaborated above, the traditional

state-of-the-art methodology is considerably bridge specific and would result in intractable number of simulations while deriving fragility curves for 509 bridges in the network. This also highlights the potential advantage of proposed parameterized fragility models pertaining to their ability to efficiently generate fragility curves by integrating out the critical bridge parameters depending on application and data availability.
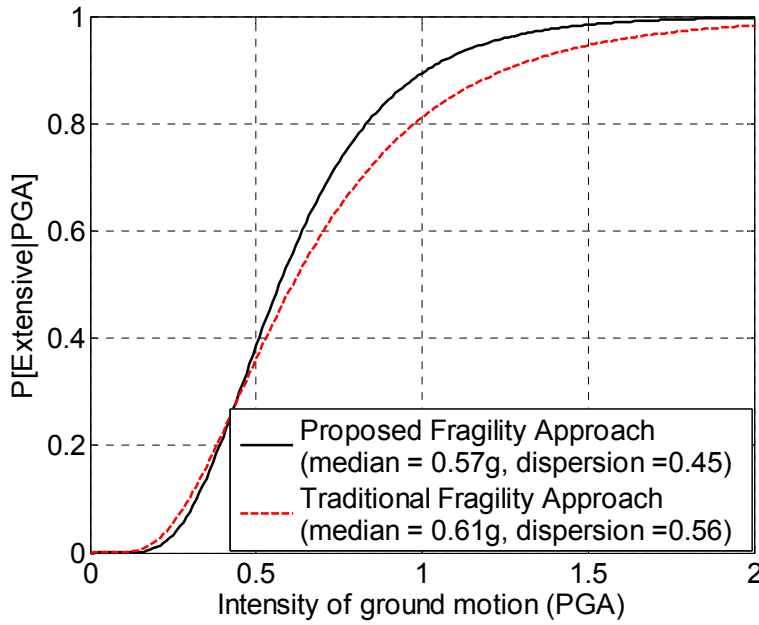

Figure 5. Comparison of fragility curve obtained using the proposed parameterized fragility approach and traditional fragility approach for case study MSSS Concrete girder bridge

Using the proposed parameterized fragility approach, the resulting fragility curve is found to have median and dispersion values of 0.57g and 0.45, while the traditional fragility methodology yields median and dispersion values of 0.61g and 0.56, respectively (Figure 5). Although median values differ only by 6.5%, the dispersion values vary significantly by almost 25%. The reduced dispersion value of the fragility curve obtained using the proposed approach can be attributed to the improved fit of the multi-dimensional surrogate demand models to component responses. These surrogate models benefit from extra predictors (x_1 to x_7) in addition to *im* which lead to better approximation to component responses as compared to single-parameter demand models (conditioned only on *im*) in the state-of-the-practice fragility methodology.

Similar conditioned-on-*im*-only fragility curves, for the extensive damage state are developed in this study for all 509 bridges in the case study network after incorporating the effects of aging

and degradation by multi-dimensional integration, which concludes Stage A of the BRAN methodology. The median and dispersion values of the fragility curves for the 509 bridges are available in the supplemental materials. Point estimates of failure probability are identified for each bridge in the network from the fragility curves and PGA at each bridge site (Figure 1). These failure probabilities are used to assess network-level reliability in Stage B.

REALIZATION OF CORRELATED BRIDGE FAILURES

Stage B of the BRAN methodology evaluates the bridge network reliability while explicitly including correlations among bridge failure probabilities. The extra correlations, as described in the companion *Methodology* paper, refer to correlations stemming from similarities among structural vulnerability of bridges which are not included in bridge structural models, as well as from the topological characteristics of bridge networks. Some factors that induce extra correlations include similarities in structural design, construction material properties, construction methods, specific site characteristics, traffic flows, maintenance strategies, and bridge network topology. The extra correlations, therefore, compensate for the impact of identified factors which are not explicitly included in bridge models of Stage A on simultaneous bridge failures.

The BRAN framework offers the necessary algorithms to simulate samples from the d-dimensional binary random variable with mean $\boldsymbol{\mu} = [P_1, P_2, ..., P_d]^T$ and correlation matrix $\boldsymbol{R}$, where d is the number of correlated bridges in the network out of the total n bridges. Correlated bridges have a failure probability between 0.05 and 0.95, as detailed in the companion *Methodology* paper. The case study network has 117 bridges (out of 509) with correlated failure probabilities, constituting 23% of the total. The remaining 392 bridges (77%) either have extremely high (110 bridges) or extremely low (282 bridges) failure probabilities which make them independent. While Stage A of the BRAN methodology provides the bridge failure probabilities (P_i's), estimating the correlation ratios among failures to set up $\boldsymbol{R}$ must depend on network owners' discretion and the availability of data in lack of explicit correlation assessments in existing post-earthquake reconnaissance reports. Accordingly, the estimated correlations may not accurately represent the actual correlation values, and therefore, a sensitivity analysis with

various levels of correlations among bridge failures is used in this paper to investigate the impact of extra correlations on network reliability estimates.

This paper evaluates the parameters contributing to extra correlations from available data on bridge structural conditions and network characteristics. In particular, the correlation matrix is set up from three sources: the current condition ratings of bridges from inspection records, the Functional Road Class (FRC) of the route the bridges are carrying, and the topological characteristics of the bridge network. This section describes the procedure of constructing the correlation matrix (R) from these three sources (the original estimate) as well as deriving correlation matrices with different values for sensitivity analysis.

The condition ratings of bridge structures from (FHWA 2010) are qualitative scores (from 0 at worst to 10 at best) assigned to bridges based on structural condition by bridge inspectors. The FRC refers to the classification of the roads carried on bridges, and is adopted from TELEATLAS highway maps (Table 7). Finally, the topological characteristics of the highway network refer to the indices that characterize its topology as a graph. The bridge network is topologically represented by a graph in which bridges (nodes) are connected by highway segments (links). Network science offers metrics to evaluate the level of topological similarities between pairs of nodes in a network, among which a degree-based similarity metric, the degree assortativity, is used in this study since it directly provides a correlation ratio. The degree assortativity establishes pair-wise bridge correlations based on the node degree (i.e. the number of highway segments directly connected to a bridge), and the similarity of their immediate neighboring bridges. The evaluated similarity between two nodes within the network is compared to that in a random network where connections are arbitrary.

The effects of corrosion and environmental agents on bridge failure probabilities are already considered in bridge structural models, and therefore, the evaluated bridge failure probabilities (Stage A) are conditionally independent of them. The three mentioned proxy data sources, on the other hand, can represent the majority of unaccounted for factors in extra correlations among bridge failures. For instance, the effects of construction methods and maintenance are reflected in the condition ratings of bridges; and a combination of bridge condition ratings and the FRC may represent the impacts of traffic loading. The correlations among bridges stemming from the

network topology (such as the degree assortativity) may indicate patterns for long term maintenance and retrofit prioritization. Specifically, the topological metric is a better predictor of the level of correlations than the geo-location of the bridges for factors such as live traffic loading, allocation of maintenance segments to contractors, etc. since topology concerns with connectivity of bridges while close by bridges may not be directly connected or even accessible from one another. In addition, the topological metrics may capture sources of correlation not yet modeled or even unknown to analysts as topology influences network functionality.

Stage B.i of the BRAN methodology sets up separate correlation matrices from bridge condition ratings (R_1), the FRC data (R_2), and the degree assortativity (R_3) before combining them to establish the overall correlation matrix (R). Forming R_3 is straightforward, while establishing R_1 and R_2 requires additional steps. The degree assortativity is equivalent to the Pearson correlation coefficient among node degrees, as described by Equation 3 (Newman 2010):

$$r_{ij} = \frac{\sum_k (A_{ik} - \bar{A}_i)(A_{jk} - \bar{A}_j)}{\sqrt{\sum_k (A_{ik} - \bar{A}_i)^2}\sqrt{\sum_k (A_{jk} - \bar{A}_j)^2}} \tag{3}$$

where r_{ij} is the similarity metric's value between nodes i and j, and $\bar{A}_i$ denotes the mean value of the ith row of the adjacency matrix. The value of r varies in [-1, 1], presenting a correlation ratio that is readily applicable to form the topological correlation matrix.

Correlation ratios in R_1 and R_2 are informed by the National Bridge Inventory and TELEATLAS databases, respectively, and require a function to transform the perceived similarities between two bridges into a correlation ratio. To be consistent with the existing research which generally prefers an exponentially decaying function (e.g. Bocchini and Frangopol, 2011), this study elects a function in the form of Equation 4, reflecting user discretion rather than real data analysis:

$$R_{q,ij} = ae^{-b(\delta_{q,ij})^2} + c \quad q = 1,2 \text{ and } i, j = 1,...,d \tag{4}$$

where $R_{q,ij}$ is the correlation ratio between bridges i and j in constituent matrix R_q; $\delta_{q,ij}$ is the difference in values associated with those bridges (in condition rating or the FRC); and a, b, and

c are model parameters to be estimated. Equation 4 maps the difference between bridges' condition ratings or FRCs into the [-1, 1] range. Parameters *a*, *b*, and *c* are evaluated by the following procedure: First, initial values of $R_{q,ij}$ (in [-1, 1]) are assumed for different δ_{ij}'s based on user's discretion on the level of correlations between bridges with various levels of similarities. Then, a function in the form of Equation 4 is fitted to the initial values by the Least Square Error method. Figure 6 demonstrates the initial values assumed in this study and the fitted curves to evaluate the entries of R_1 and R_2. For instance, Figure 6b associates the maximum and minimum differences in the FRC levels with correlation ratios of -0.4 and 1, respectively. The fitted function reduces correlation levels at the limits to -0.33 and 0.83.

Table 7. Functional Road Classes (FRCs) as per TELEATLAS classification

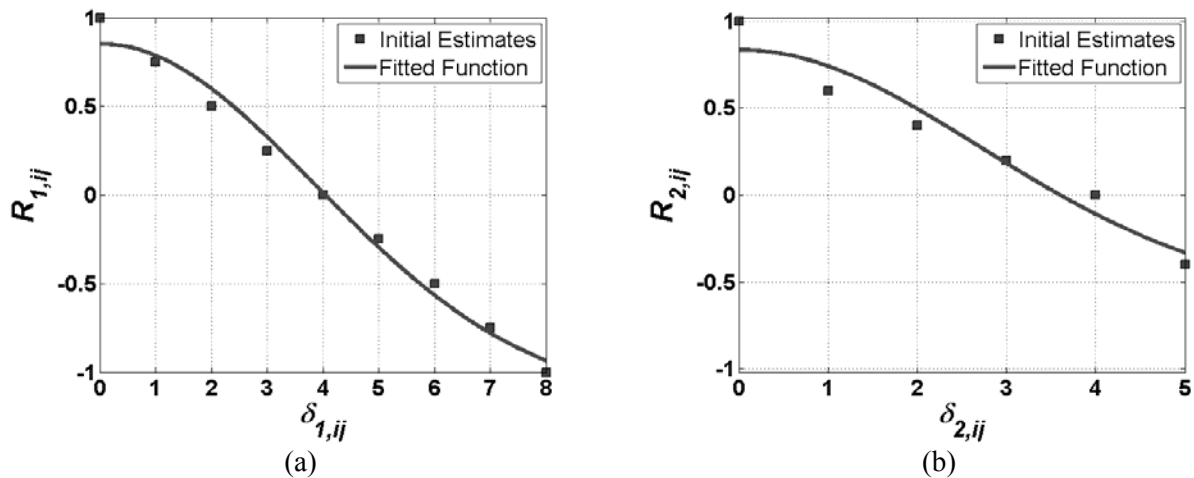| FRC	Description
0	Motorway, freeway, or other major road
1	A Major road less important than a motorway
2	Other major road
3	Secondary road
4	Local connecting road
5	Local road of high importance

(a)   (b)

Figure 6. Estimated correlation ratios between bridges *i* and *j* for a) the difference in condition ratings, and b) the difference in the Functional Road Class. The differences between the condition ratings in the NBI database vary from 0 to 8, while the FRCs differ by 0 to 5 levels (Table 7). The fitted function is

derived by Equation 4 fitted to the initial estimates.

The correlation ratios from the three constituent matrices are not final yet, as they must be examined for compatibility with the failure probabilities of bridges. The width of the admissible range of correlation ratios between two bridges is a function of the difference between their failure probabilities, with larger differences resulting in a narrower admissible range of correlation ratios. The same admissible ranges apply to all three constituent matrices since the ranges solely depend on bridge failure probabilities. Two auxiliary matrices, R_{min} and R_{max}, store the minimum and maximum allowable correlation ratios, respectively, and all elements $R_{q,ij}$ are transformed to the admissible range $[R_{min}(i,j), R_{max}(i,j)]$, as elaborated in the companion *Methodology* paper. The modified constituent correlation matrices are now ready to combine and form the compatible correlation matrix R_0', where the zero subscript denotes the compatible correlation matrix is mapped from the originally estimated correlation values. The user has the flexibility of choosing the desired combination as well as weights to establish the correlation matrix. In the absence of further information on the relative importance of the three sources on correlation levels, this research assigns equal importance to the constituent matrices, and consequently, establishes the modified correlation matrix as their average. This modified correlation matrix can be used alongside bridge failure probabilities to simulate realizations of correlated bridge failures.

For sensitivity analysis, other compatible correlation matrices are derived by varying the originally estimated correlation matrix. The companion *Methodology* paper presents the formulation of the varied correlation matrices R_λ', where positive and negative λ values represent the shift of correlation ratios towards R_{max} and R_{min}, respectively. For example, $\lambda = 0.4$ denotes that all correlation ratios are shifted towards their respective values in R_{max} by 40%. For this case study, λ values vary from -0.5 to 0.5 in 0.1 intervals, producing a total of eleven correlation matrices for network reliability analysis.

The normalized error metric (E) introduced in the companion *Methodology* paper measures the level of changes in the correlation ratios in the modification process. For the original estimates in R_0', E is computed to be 5%. The small produced error supports the choice of the

three information sources to establish the correlation matrix. Although correlation ratios are not estimated based on real post-earthquake data analysis, they at least show reasonable compatibility with bridge failure probabilities. Nevertheless, it must be noted that compatibility does not necessarily imply accuracy of estimates. Therefore, the impact of varying correlation levels on network reliability is investigated in the sensitivity analysis offered in the next section.

SIMULATING BRIDGE FAILURE REALIZATIONS

The companion *Methodology* paper describes the Dichotomized Gaussian Method (DGM) to simulate realizations of bridge failures from their correlated failure probabilities and the modified correlation matrix. DGM forms a covariance matrix (S) for an associated d-dimensional (here, $d = 117$) normal random variable. The normal random variable is used as a proxy to generate realizations from the d-dimensional binary random variable. This research employs package *Bindata* (Leisch et al. 1998) in the statistical analysis software R (R Development Core Team 2010) to establish matrix S. In high dimensional problems such as this case study, evaluating this matrix often incurs numerical errors (e.g. from numerical integration). Moreover, and since satisfying the compatibility conditions does not guarantee the modified correlation matrix to be strictly positive-definite, the computed matrix S may have a few small negative eigenvalues. A straightforward routine to solve this problem is setting the erroneously produced negative eigenvalues of S equal to zero in its eigenvalue decomposition. Realizations from the d-dimensional binary random variable are subsequently simulated by the same software package. The remaining 392 bridges with independent failures do not require Stages B.i and B.ii of the BRAN methodology to simulate correlated failure samples, and their failure samples are simulated independently. To increase the efficiency of computations, independent failures are generated using quasi random numbers rather than common pseudo-random number generators. This research uses the Sobol sequence to generate quasi random numbers for its superior performance in high dimensional problems (Morokoff and Caflisch 1995; Boyle et al. 1997). To conclude Stage B, realizations of correlated bridge failures are combined with independent failure realizations to form a data-frame consisting of N_{MC} realizations of the n-dimensional binary random variable. For sensitivity analysis, eleven data-frames are generated corresponding to the shifted correlation matrices R'_λ, $\lambda = -0.5, ..., 0.5$. The data-frames are used to evaluate the network reliability by the modified MCMC.

RESULTS AND DISCUSSIONS

Figure 7 shows the frequency distribution of the failure probabilities corresponding to the 509 bridges in the network. Evidently, the majority of the bridges have extreme failure probabilities. A significant percentage of the bridges with very low failure probabilities are comprised of MSSS Slab, MSC Slab, SS Concrete, and SS Steel bridges which are found to be relatively non-vulnerable to the scenario seismic event owing to minimal bearing deformations and low column demands (for multi- span bridges) The low seismic vulnerability of these bridge types is in agreement with similar findings by Rokneddin et al. (2011). Bridges with high failure probabilities tend to belong to the aging MSC Steel, MSSS Steel, and MSSS Concrete girder bridge classes characterized by high demands on column, bearing and abutment deformations and are primarily concentrated near the epicenter characterized by high PGA intensity.
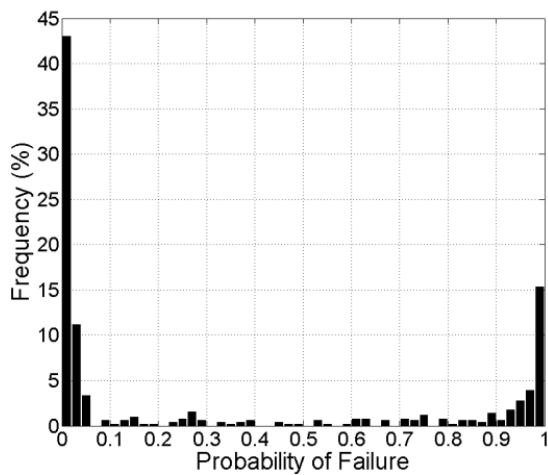

Figure 7. Frequency distribution of the failure probabilities corresponding to the 509 bridges in the chosen case study network.
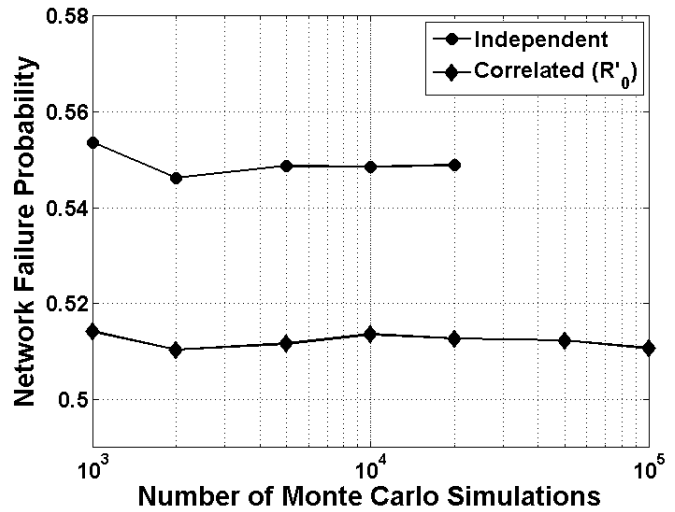
Figure 8. Network connectivity reliability between origin and destination nodes versus the number of samples in Monte Carlo simulations.

The network-level reliability objective in this study is to maintain connectivity between the origin and destination nodes depicted in Figure 1. The defined objective is concerned with the accessibility of populated areas of the city from the outside area for relief actions after a major earthquake such as the considered scenario. Figure 8 compares the network reliability estimates

as a function of the number of Monte Carlo simulations. Both independent and correlated (based on original estimates R'_0) bridge failures are examined, and the simulations continue until the standard deviation of estimates falls below 0.005. The Independent scenario shows superior efficiency as it benefits from quasi-Monte Carlo sampling, and only requires up to 20,000 simulations. The correlated scenario, on the other hand, needs 100,000 simulations. Figure 8 suggests that the original estimates for extra correlations among bridge failures improve the reliability of the case study network by reducing its failure probability from around 0.55 to 0.51.

Figure 9 presents the results of the sensitivity analysis, along with the associated error E for each R'_λ. Figure 9(a) suggests that overall, more positive correlations improve the reliability of the case study network. On the other hand, the failure probability generally increases as λ moves towards negative values before dropping at λ = -0.5. In spite of this increase, the failure probability does not reach that of the independent scenario. The range of failure probability variations is around 20% of the failure probability associated with the original estimates (0.51), which emphasizes the impact of extra correlations and underlines the need to develop post-earthquake-data-driven models to better estimate the extra correlations. Figure 9(b) shows that the error associated with R'_λ stabilizes for more positive correlates and sharply increases for more negative correlation levels; suggesting that correlation values less than the original estimates would be far less compatible with bridge failure probabilities.
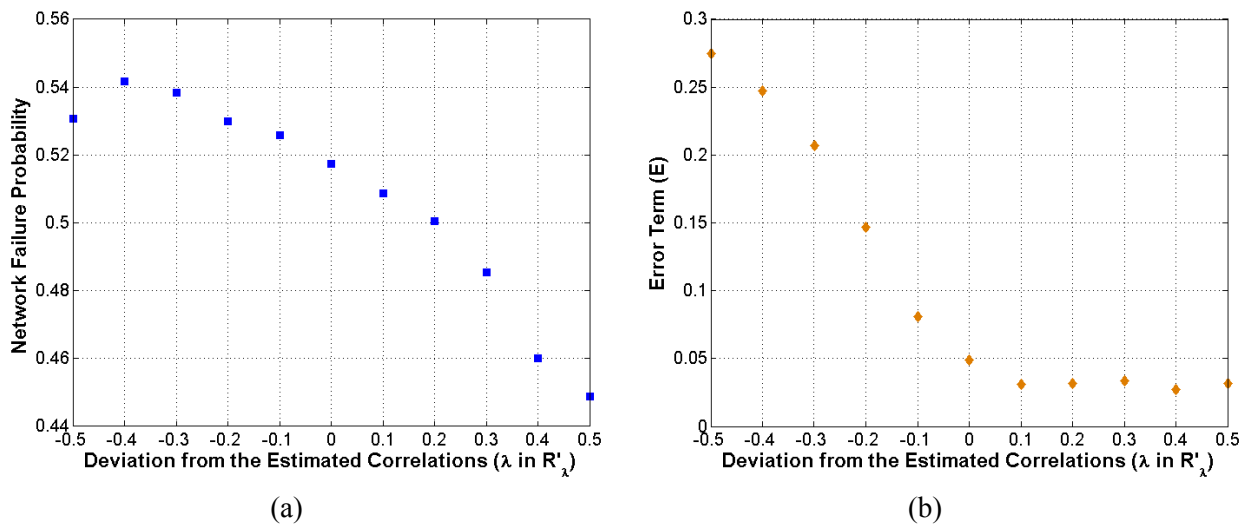

(a)   (b)

Figure 9. The impact of varying λ on: a) the probability of failure in the case study network, and b) the

error term associated with R'_λ by compatibility modifications.

Several past studies on the seismic reliability of bridge networks have suggested that neglecting correlations results in underestimation of losses at the network level (e.g. Bommer and Crowley (2006) and Lee and Kiremidjian (2007)). It is important to note that those studies have considered different types of correlations (hazard intensities in terms of inter- and intra-event errors, and seismic response of structures) and present the results for a different limit state (loss in monetary terms rather than network connectivity). Neglecting the spatial correlations resulting from of inter- and intra-event error terms is commonly assumed to underestimate the assessed loss in a portfolio of structures. However, for the network connectivity reliability with extra correlations, the impact depends on the correlation signs and the topology of the network, and may vary among different networks.

To further investigate the impact of extra correlations on network reliability assessments, two different scenarios are studied in which the origin and destination nodes have changed to produce tail failure probabilities in the case study network. Figure 10 presents the results of the sensitivity analysis on the failure probability of these scenarios with the same range of λ values as before. To be consistent with the original case study, the simulations continue until the standard deviation of reliability estimates reaches 0.005. As expected, the extra correlations have far less influence on extreme failure probabilities.
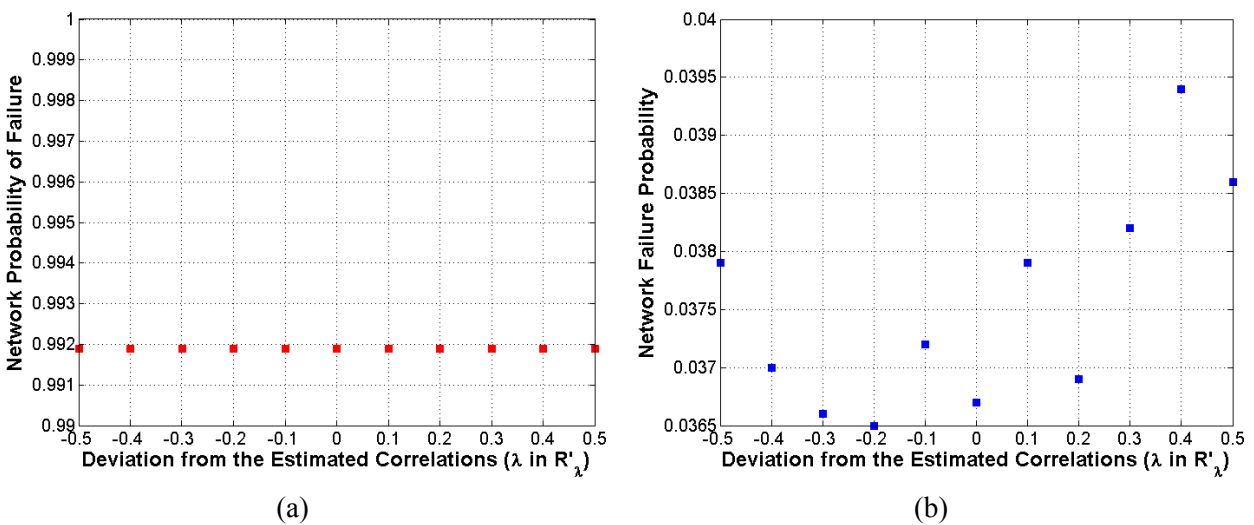

(a)   (b)

Figure 10. The impact of varying λ on the network failure probability with: a) an origin-destination pair

resulting in extremely high failure probability, and b) an origin-destination pair resulting in a very low probability of failure.

The significance of incorporating field instrumentation data is also examined by comparing bridge failure probabilities in Figure 7 with those obtained without updating historical deterioration parameters. For the original case study example, bridge failure probabilities are found to be underestimated or overestimated by as much as 115% and 55%, respectively. Additionally, more than 80% of bridge failure probabilities change by ± 25% when field instrumentation data is not incorporated in the case study network. At the network level, the probability of failure for the three-source correlation structure reduces from 0.51 to 0.45 when updating of historical deterioration estimates is not implemented.

CONCLUSIONS

This paper presents a case study application of the two-stage bridge reliability assessment in networks (BRAN) methodology. Part of the highway bridge network in South Carolina, USA, is studied under a large seismic scenario for network-level connectivity reliability between selected origin and destination points. The aging 509 bridges in the network are categorized into nine different bridge classes depending on material and bridge type. Bridge failure probabilities are estimated using a parameterized fragility formulation and hypothetical deterioration parameter data obtained from field instrumentation and spatial interpolation. Since all factors influencing the simultaneous failure of bridges in seismic scenarios are not integrated into the bridge structural modeling, correlations among bridge failure probabilities (i.e., extra correlations) are estimated and incorporated in the assessment of the case study bridge network reliability. In lack of post-earthquake-data-driven models to evaluate the correlations among bridge failure probabilities, three sources of information (i.e., bridge condition ratings, functional road classes, and the network topology) are employed to estimate the extra correlations and form the correlation matrix. The correlation matrix is modified for compatibility with bridge failure probabilities and used to generate correlated bridge failure realizations, which are finally used in a modified Markov Chain Monte Carlo simulation framework to estimate the network reliability.

Several bridge classes, especially slab type and simply supported bridges, are relatively non-vulnerable to seismic events due to low seismic demands on bearings and columns. On the

contrary, proximity to the epicenter of the earthquake makes many bridges highly vulnerable. Therefore, the majority of bridges (77%) in the network have either extremely high or low probabilities which make their failures independent. Forming the overall correlation matrix for the remaining 23% requires modifications for compatibility with bridge failure probabilities, which result in a relative change in the final correlation matrix two-norm of approximately 5%. The impact of different correlation levels on the reliability of the case study network is investigated by a sensitivity analysis with shifting the estimated correlations ratios towards their minimum and maximum admissible values. Network reliability simulations reveal that more positive correlations generally improve the connectivity reliability in the case study network, resulting in up to 0.09 increase in the network reliability where the network failure probability without accounting for correlations is around 0.54. This finding does not contradict the existing literature on the assessment of losses to a portfolio of structures, since those assessments consider different limit states such as the level of loss in monetary terms. The best-estimate correlation matrix which is established from the three information sources is also found to improve the network reliability by around 0.03 over the independent case. The impact of extra correlations on network connectivity reliability is a function of the signs of correlation ratios as well as the network topology, and may vary among different networks. The importance of incorporating deterioration parameter data from field instruments is also emphasized. The case study reveals that some bridge failure probabilities are either underestimated or overestimated by as large as 115% and 55% when only historical estimates of deterioration parameters are used. Moreover, network reliability assessment by ignoring field instrumentation data underestimates the reliability of the case study network by 0.06.

The aim of the BRAN methodology is to present a comprehensive approach that integrates the parameterized aging bridge fragility modeling with enhanced Monte Carlo based network reliability analysis in highway bridge networks. The framework is general enough to incorporate improvements in the future, such as more advanced surrogate demand models and flow-based network reliability objectives. Critical bridges in transportation networks for retrofit prioritization and other actions can be identified from network reliability results of BRAN. Opportunities for future work exist in investigating propagation of uncertainty at various stages of the BRAN methodology as well as simultaneously accounting for inter- and intra-event correlation terms in a probabilistic seismic hazard analysis.

ACKNOWLEDGEMENTS

REFERENCES

Ang, A.H.-S. & Tang, W.H., 2007. *Probability concepts in engineering*, Wiley.

ASCE, 2009. ASCE: Infrastructure Fact Sheet. Available at: http://www.infrastructurereportcard.org/sites/default/files/RC2009_bridges.pdf.

Atkinson, G.M. & Boore, D.M., 1995. Ground-motion relations for eastern North America. *Bulletin of the Seismological Society of America*, 85(1), pp.17–30.

Board, N.R.C. (U. S.). G., Institute, E.E.R. & (U.S.), N.R.C., 1994. *Practical lessons from the Loma Prieta earthquake: report from a symposium sponsored by the Geotechnical Board and the Board on Natural Disasters of the National Research Council : symposium held in conjunction with the Earthquake Engineering Research Institute ... [et al.].*, National Academies.

Bocchini, P. & Frangopol, Dan M., 2011. A stochastic computational framework for the joint transportation network fragility analysis and traffic flow distribution under extreme events. *Probabilistic Engineering Mechanics*, 26(2), pp.182–193.

Bommer, J.J. & Crowley, H., 2006. The Influence of Ground-Motion Variability in Earthquake Loss Modelling. *Bulletin of Earthquake Engineering*, 4(3), pp.231–248.

Boyle, P., Broadie, M. & Glasserman, P., 1997. Monte Carlo methods for security pricing. *Journal of Economic Dynamics and Control*, 21(8-9), pp.1267–1321.

Campbell, K.W., 2003. Prediction of strong ground motion using the hybrid empirical method and its use in the development of ground-motion (attenuation) relations in eastern North America. *Bulletin of the Seismological Society of America*, 93(3), pp.1012–1033.

Chang, S.E., 2000. Disasters and transport systems: loss, recovery and competition at the Port of Kobe after the 1995 earthquake. *Journal of Transport Geography*, 8(1), pp.53–65.

Choi, E., DesRoches, Reginald & Nielson, B., 2004. Seismic fragility of typical bridges in moderate seismic zones. *Engineering Structures*, 26(2), pp.187–199.

Cornell, C. A., Fatemeh, J., Hamburger, R.O., Foutch, D.A., 2002. Probabilistic Basis for 2000 SAC Federal Emergency Management Agency Steel Moment Frame Guidelines. *Journal of Structural Engineering*, 128(4), pp.526–533.

Enright, M.P. & Frangopol, Dan M., 1999. Condition Prediction of Deteriorating Concrete Bridges Using Bayesian Updating. *Journal of Structural Engineering*, 125(10), pp.1118–1125.

Enright, M.P. & Frangopol, Dan M., 1998. Probabilistic analysis of resistance degradation of reinforced concrete bridge beams under corrosion. *Engineering Structures*, 20(11), pp.960–971.

FEMA, 2009. FEMA Library - HAZUS®MH MR4 Earthquake Model User Manual. Available at: http://www.fema.gov/library/viewRecord.do?id=3732 [Accessed March 11, 2011].

FHWA, 2010. NBI ASCII Files - NBI - Programs - Integrated - Bridge - FHWA. Available at: http://www.fhwa.dot.gov/bridge/nbi/ascii.cfm?year=2010 [Accessed March 11, 2011].

Frangopol, D.M., Lin, K.Y. & Estes, A.C., 1997. Reliability of reinforced concrete girders under corrosion attack. *Journal of Structural Engineering*, 123(3), p.286.

Frankel, A.D. et al., 2002. *Documentation for the 2002 update of the national seismic hazard maps*, US Department of the Interior, US Geological Survey. Available at: https://geohazards.usgs.gov/trac/export/152/NSHMP/trunk/docs/NSHM-2002-OFR02-420.pdf [Accessed October 31, 2012].

Funahashi, M.I., 1990. Predicting corrosion-free service life of a concrete structure in a chloride environment. *ACI Materials Journal*, 87(6).

Ghosh, J. & Padgett, J.E., 2010. Aging Considerations in the Development of Time-Dependent Seismic Fragility Curves. *Journal of Structural Engineering*, 136(12), pp.1497–1511.

Ghosh, J. & Padgett, J.E., 2012. Impact of Multiple Component Deterioration and Exposure Conditions on Seismic Vulnerability of Concrete Bridges. *Earthquakes and Structures*, In Press.

Han, Q., Xiuli, D., Jingbo, L., Zhongxian, L., Liyun, L., Jianfend, Z., 2009. Seismic damage of highway bridges during the 2008 Wenchuan earthquake. *Earthquake Engineering and Engineering Vibration*, 8(2), pp.263–273.

Kim, S.H. & Shinozuka, M., 2004. Development of fragility curves of bridges retrofitted by column jacketing. *Probabilistic Engineering Mechanics*, 19(1), pp.105–112.

Lee, R. & Kiremidjian, A.S., 2007. Uncertainty and Correlation for Loss Assessment of Spatially Distributed Systems. *Earthquake Spectra*, 23(4), p.753.

Leisch, F., Weingessel, A. & Hornik, K., 1998. On the generation of correlated artificial binary data.

Liam, K., Roy, S. & Northwood, D., 1992. Chloride ingress measurements and corrosion potential mapping study of a 24-year-old reinforced concrete jetty structure in a tropical marine environment. *Magazine of Concrete Research*, 44(160), pp.205–215.

Mackie, K.R. & Stojadinovic, B., 2006. Post-earthquake functionality of highway overpass bridges. *Earthquake Engineering & Structural Dynamics*, 35(1), pp.77–93.

Morokoff, W.J. & Caflisch, R.E., 1995. Quasi-monte carlo integration. *Journal of Computational Physics*, 122(2), pp.218–230.

Mustafa, M. & Yusof, K., 1994. Atmospheric chloride penetration into concrete in semitropical marine environment. *Cement and Concrete Research*, 24(4), pp.661–670.

Newman, M.E.J., 2010. *Networks: an introduction*, Oxford University Press.

Nielson, B.G., 2005. *Analytical fragility curves for highway bridges in moderate seismic zones*. PhD Thesis. Atlanta, Georgia: Georgia Institute of Technology.

Nielson, B.G. & DesRoches, R., 2007. Analytical Seismic Fragility Curves for Typical Bridges in the Central and Southeastern United States. *Earthquake Spectra*, 23(3), pp.615–633.

Padgett, J.E. & DesRoches, R., 2009. Retrofitted bridge fragility analysis for typical classes of multispan bridges. *Earthquake Spectra*, 25(1), pp.117–41.

Padgett, J.E., DesRoches, R. & Nilsson, E., 2010. Regional Seismic Risk Assessment of Bridge Network in Charleston, South Carolina. *Journal of Earthquake Engineering*, 14(6), pp.918–933.

R Development Core Team, 2010. The R Project for Statistical Computing. Available at: http://www.r-project.org/ [Accessed December 30, 2011].

Rokneddin, K., Ghosh, J., Dueñas-Osorio., L., Padgett, J., 2011. Bridge retrofit prioritization for aging transportation networks subject to seismic hazards. *Structure and Infrastructure Engineering*, In Press.

Schiff, A.J., 1995. *Northridge earthquake: lifeline performance and post-earthquake response*, ASCE Publications.

Shome, N. & Cornell, C. A, 1999. *Probabilistic Seismic Demand Analysis of Nonlinear Structures*, Stanford, California: Stanford University.

Suzuki, M., Tsutsumi, T. & Irie, M., 1990. Reliability analysis of durability/deterioration indices of reinforced concrete in a marine environment. *Corrosion of Reinforcement in Concrete*, pp.268–277.

TELEATLAS, 2010. Digital Mapping and Navigation Soultions. Available at: http://www.teleatlas.com/index.htm.

Thoft-Christensen, P., 1995. Advanced bridge management systems. *Structural Engineering Review*, 7(3), pp.151–164.

Toro, G.R., Abrahamson, N.A. & Schneider, J.F., 1997. Model of Strong Ground Motions from Earthquakes in Central and Eastern North America: Best Estimates and Uncertainties. *Seismological Research Letters*, 68(1), pp.41–57.

Trauth, M.H., Gebbers, R. (CON) & Marwan, N. (CON), 2010. *MATLAB® Recipes for Earth Sciences*, Springer.

Uji, K., Matsuoka, T. & Maruya, T., 1990. *Corrosion of Reinforcement in Concrete*, London: Elsevier.

USGS, 2010. USGS Interactive Deaggregations Maps. Available at: http://eqint.cr.usgs.gov/deaggint/2008/index.php [Accessed March 11, 2011].

Val, D.V., Stewart, M.G. & Melchers, R.E., 1998. Effect of reinforcement corrosion on reliability of highway bridges. *Engineering Structures*, 20(11), pp.1010–1019.

Vu, K.A.T. & Stewart, M.G., 2000. Structural reliability of concrete bridges including improved chloride-induced corrosion models. *Structural Safety*, 22(4), pp.313–333.

Webster, R. & Oliver, M.A., 2008. *Geostatistics for Environmental Scientists*, John Wiley & Sons.

Wong, I., Bouabid, J., Graf, W., Huyck, C., Porush, A., Silva, W., Siegel, T., Bureau, G., Eguchi, R., Knight, J., 2005. Potential losses in a repeat of the 1886 Charleston, South Carolina, Earthquake. *Earthquake spectra*, 21, p.1157.

Zen, K., 2005. Corrosion and life cycle management of port structures. *Corrosion science*, 47(10), pp.2353–2360.